RSC Advances

ROYAL SOCIETY OF CHEMISTRY

www.rsc.org/advances

Self-doped 3-hexylthiophene-*b*-sodium styrenesulfonate block copolymer: Synthesis and its organized with CdSe quantum dots

Jin Wang*[a], Chenchen Guo[a], Yongqiang Yu[b], Huabing Yin[c], Xueting Liu[a] and Yang Jiang[d]

[a] *School of Chemistry and Chemical engineering, Hefei University of Technology, Hefei 23009, P. R. China. E-mail: jinwang@hfut.edu.cn*

[b] *School of Electronic Science and Applied Physics, Hefei University of Technology, Hefei 23009, P. R. China.*

[c] *Department of Electronics and Electrical Engineering, University of Glasgow, G12 8QQ, UK.*

[d] *School of Materials Science and Engineering, Hefei University of Technology, Hefei 23009, P. R. China.*

Abstract：A new self-doped 3-hexylthiophene-*b*-Sodium styrenesulfonate block copolymer (P3HT-*b*-PSSNa) was obtained via solution copolymerization of styrene sulfonate (SSNa) with vinyl end group poly (3 - hexylthiophene) (*v*-P3HT) which synthesized under Grignard metathesis (GRIM) reaction conditions. The self-doping structure can be controlled by altering the feed amounts of SSNa monomer, and exhibits tunable properties. In compassion with *v*-P3HT, P3HT-*b*-PSSNa shows good solubility, broad absorption, higher electrical conductivity and well donor/acceptor (D/A) interface binding with CdSe quantum dots (QDs). The composites of P3HT-*b*-PSSNa and CdSe show a uniform dispersion, good compatibility and highly efficient fluorescence quenching, and the surface chemical state analysis verified the chemical bonding between copolymer and QDs. This is help for the fast charge transfer of different semiconductors in the two-phase D/A interface. Here we developed a strategy for producing conjugated polymer with both doped stability during repeated electric cycle and compatibility with inorganic semiconductor materials.

Keywords：block copolymer; self-doped; P3HT-*b*-PSSNa; CdSe

Introduction

Polythiophene derivatives have been widely concerned due to their good electrical properties and stability, and regioregular poly (3-alkylthiophene)s (rrP3ATs) are some of the most widely studied conducting polymers. The Grignard metathesis[1] (GRIM) evolved by McCullough provide a simple and economical method for rrP3ATs, and much of recent research and commercial products in polymer organic electronics or photoelectronics were based on rrP3ATs. Potential and practical applications include chemical and optical sensors, electrochromic devices, field effect transistors, and solar cells.[2-5]

Conjugated polymers with the extended π-electron system exhibit a pseudo-bandgap in the range of 1.5～2.5 eV, and have low conductivity and mobility.[6] Generally, the conductivity of these undoped conjugated polymers is 10^{-7}～10^{-11} S cm^{-1}. But for the application of conjugated polymers instead of inorganic or traditional semiconductors some higher conductivity is required. Doping is an effective method to produce conducting polymers. In contrast to inorganic semiconductor systems, doping in the case of conjugated polymers refers to the oxidation or reduction of the π-electronic system, p-doping and n-doping, respectively. The polymers having conjugated double bonds can be oxidized or reduced using charge transfer agents (dopant) more easily for better electrochemical activity.

The issue for doped conductive polymers at the present time is their relative instability under atmospheric conditions. The use of external dopant whose stabilities have always been a problem associated with many practical applications, especially under thermal and electric cycle applications. Self-doping in conducting polymers has been proved that can improve the stability upon cycling in neutral and alkaline.[7] Self-doped polyanilines (PAns) have been studied extensively. It involves the small molecule acidic group internal doping such as fuming sulfuric acid treatment PAn,[8] and copolymer of acid and aniline such as poly (aniline-co-N-benzoylsulfonic aniline) which obtained by post-synthesis treatment of PAn in the presence of o-sulfobenzoic anhydride.[9] The self-doping of polythiophene and its derivatives were also explored. Banahalli Ratna[10] had synthesized poly (thiophene-3-oligoethylene glycol sulfonate) which obtained by incorporating long sulfonate-terminated tethers into the conducting polymer polythiophene, and had reversible doping and dedoping effect. The sulfonated polythiophene derivative poly [2-(3-sulfinopropyl)-2,3-dihydro-thieno [3,4-b][1,4] dioxin] was synthesized from (3,4-ethylenedioxythiophene) sulfonate monomer in the present of $FeCl_3$.[11] Due to the immobilization of sulfonated group

covalently linked, the thin polymer films were shown to be highly stable in air in their doped state on the contrary to the thiophene derivatives. In brief, people have recognized that the nature of interaction between dopant and conjugated polymer has a strong influence on the stabilization at the doped state. The chemical bonding such as include hydrogen bonding, covalent bonding, and coordination bonding are benefit for the stability although they may does not further extent the electroactivity.

Another issue of conducting polymer is concerned widely is their solubilities from the real application point of view. The grafting of pendant side groups onto the polymer backbone such as a flexible alkyl chain, alkoxy groups has also been investigated in order to enhance its solubility.[12-14] However, researchers have observed that the presence of alkyl constituent groups on the conducting polymer unit increases the solubility but decreases the conductivity. Polythiophene derivatives such as P3HT just dissolved in the limited organic solvents such as chloroform. Which are not good for the blend with inorganic semiconductor when used for hybid heterojunction. It had been reported that the sulfonic acid groups ($-SO_3^-$) were added into conjugated polymeric backbone to form the self-doped copolymer have better solubility and its photoelectric performance was improved after film-forming.[15,16] Polythiophene derivatives also incorporate with inorganic semiconductors to form active materials for photoelectronics applications.[17-19] In a inorganic-organic hybrid photoelectron conversion devices, one limitation to the efficiency is the electron transfer from an excited-state of a donor polymer to an inorganic electron acceptor material. A possible nanoparticle aggregation often limits the energy transfer pathway and leads to the uncontrollable phase separation of both components on a micrometer scale. It is obviously that the ideal nanostructures will facilitate efficient charge photogeneration and device performance for organic semiconductors with short diffusion lengths. The relationship between nanomorphology and photophysical properties of a *in situ* grown CdS:P3HT blends has been researched,[20] and have shown that the charge generation from P3HT excitons is heavily nanomorphology dependent. In our previous research,[21] the interrelationship between D/A type 3-hexylthiophene/pyridine copolymer (P3HT/PY) and CdSe QDs was studied, and showed that the good compatibility between P3HT/PY copolymer and CdSe QDs is advantageous for the electron transfer.

In this paper, we synthesized a self-doped poly (3-hexylthiophene)-*b*-poly(styrene sulfonate) (P3HT-*b*-PSSNa) in which styrene sulfonate (SSNa) doping segments were bonded chemically with P3HT molecular chain. On the one hand, the dopant sulfonic

acid groups can improve the conductive properties of conjugated polymers greatly and formed stable and reversible redox system, on the other hand, the hydrophilic styrene sulfonate segments can improved the compatibility between thiophene polymers with inorganic semiconductor materials effectively. The good dispersion of inorganic QDs into the conjugated polymer promotes the charge transfer in their D/A interface, and accordingly increasing the photoelectric conversion efficiency in the heterojunction structure.

Experimental Section

Materials

Butylmagnesium Chloride solution(C_4H_9ClMg, 2M in THF), vinylmagnesium bromide(C_2H_3BrMg, 1M in THF), sodium styrene sulfonate (SSNa) and [1, 3-bis(diphenylphosphino)propane] dichloronickel (II) (Ni(dppp)Cl_2) (99%), cadmium oxide(CdO), selenium dioxide(SeO_2), palmitic acid, octadecylene were purchased from Aladdin Reagent Detabase Inc. Tetrahydrofuran(THF), methyl alcohol, trichloromethane, benzoperoxide(BPO) and N-methyl pyrrolidone(NMP) were purchased from Sinopharm Chemical Reagent Co.Ltd. 2,5-dibromo-3-hexylthiophene were purchased from Puyang Huicheng Electronic Material Co.Ltd. THF was purified to get anhydrous THF before used. Other reagents and medicine were used directly. All reactions were under the high purity nitrogen protection, all glasswares were dried without water.

Synthesis of *v*-P3HT

A dry three-necked flask was vacuumed with full of nitrogen, and charged with 2, 5 - dibromo-3-hexylthiophene (2.14 mL, 10 mmol) and anhydrous THF (10 mL). 5 mL C_4H_9ClMg (2M in THF) was injected by a syringe, and stirred at room temperature for 2 h. 0.1 g Ni(dppp)Cl_2 was added into quickly and stirred for 10 minutes at the room temperature, then C_2H_3BrMg(1M in THF) (2～3 mmol) and THF (10 mL) was added to the reaction mixture, continued to stir for 5 minutes then poured into methanol to precipitate the polymer at low temperature. The polymer was filtered into an extraction thimble and then washed by Soxhlet extraction with methanol, hexanes, and chloroform, respectively, and then purified by extraction with chloroform. ^{1}H NMR (500 MHz, $CDCl_3$): δ_H 6.96 (s, 1H), 6.83(m, 1H), 5.49 (d, 1H), 5.11 (d, 1H), 2.807~0.915 (m, 13H). GPC: M_n: 6575, M_w: 9051, M_w/M_n: 1.5.

Synthesis of P3HT-*b*-PSSNa

v-P3HT powder was added into dry three-necked flask, and dissolved in a suitable amount of chlorobenzene and trichloromethane mixture under nitrogen protection,

then BPO (10 to 15 mol % of monomer) was put into the flask as the initiator, stirred and heated to 70 °C slowly. Proper amount of SSNa which dissolved in NMP was added into flask by drops. The reaction mixture was stirred for 6 to 8 h at 70 °C. The final product was purified by precipitation with methanol and distilled water successively, and then filtration. The resident was then washed by distilled water and filtration. The residence was vacuum dried for 12h. Characterization of P3HT-b-PSSNa-0.2: ^{1}H NMR (500 MHz, $CDCl_3$): δ_H 8.19 (d, 1H), 8.07 (d, 1H), 7.63 (d, 1H), 7.43 (d, 1H), 6.96 (s, 1H), 3.42 (m, 1H), 2.78 (t, 2H), 1.32~1.69 (m, 4H), 1.58~0.76 (m, 13H); GPC: M_n: 7594, M_w: 11815, M_w/M_n: 1.6.

Preparation of composite films of P3HT-*b*-PSSNa/CdSe

CdSe QDs were synthesized according to the literature.[22] Composite films were prepared by turning the mass ratio of P3HT-*b*-PSSNa-0.2 and CdSe into 1:0.2, 1:0.5, and 1:1, respectively. The mixtures were ultrasonicated for 5 min at 25 °C to get a uniform liquid and then were spin-coated onto the ITO substrate.

Characterization and measurement

^{1}H NMR spectra were recorded using VNMRS600 superconducting NMR spectrometer from Agilent Technologies Group. The molecular weight of polymers were measured by gel permeation chromatography (GPC) using a 410 Waters differential refractometer at a flow rate of 1 mL/min, in which THF was used as the eluent and polystyrene as a standard. Fluorescence properties of copolymer was tested via F4500 fluorescence spectrometer from Type of Hitachi company and UV-Vis was tested by UV-2550 which from Shimadzu Group. X-ray photoelectron spectroscopy (XPS) analysis was conducted by a ThermoFisher ESCALAB250 in which the electronic binding energies of the samples were measured. Cyclic voltammetry (CV) was conducted on a CHI660B electrochemical workstation with Pt plane and Ag/Ag^+ as the working electrode, counterelectrode and reference electrode, respectively. Electrolyses were performed using a tetrabutylammonium hexafluorophosphate (Bu_4NPF_6) acetonitrile solution (0.1 M) at a scan rate of 50 mV / S.

Results and discussion

Synthesis and structure

The synthetic routes of P3HT-*b*-PSSNa are depicted in Scheme 1. *v*-P3HT was synthesized through GRIM method. Subsequently, *v*-P3HT with reactive vinyl end group copolymerized with SSNa monomer via a simple solution polymerization, and producing P3HT-*b*-PSSNa. The chemical structures of *v*-P3HT and P3HT-*b*-PSSNa were confirmed by ^{1}H NMR spectroscopy. The ^{1}H NMR spectra expansion in the

region 8.5-5 ppm for *v*-P3HT and P3HT-*b*-PSSNa are shown in Fig.1(a) and Fig.1(b), respectively. As shown in Fig.1(a), the peak at 6.96 ppm (g) is assigned to the resonance of protons on the thiophene ring with head-to-tail (HT) coupling, [23] which confirms the highly regioregular structure of *v*-P3HT. The appearance of new signals at 5.49 ppm (i) and 5.11 ppm (i) are due to the terminated vinyl protons, and signal at 6.83 ppm (h) is due to the vinyl proton which connected to thiophene ring, respectively. In comparison with the ^{1}H NMR spectrum of *v*-P3HT copolymer, the signals of vinyl proton at 5.49 ppm and 5.11 ppm have disappeared in the ^{1}H NMR spectrum of P3HT-*b*-PSSNa, the appearance of new signals at 8.19 ppm (a) and 8.07 ppm (b) in Fig.1(b) are due to the hydrogen of benzene ring on one side of the sulfonic acid group, respectively. The signals at 7.43 ppm (c) and 7.63 ppm (d) belong to the hydrogen of benzene ring on one side of the ethylidene. From the ^{1}H NMR spectra, it can be confirmed that SSNa units have been bonded with P3HT by means of reacting with vinyl end group. i.e., P3HT-*b*-PSSNa block copolymer was synthesized successful. The GPC test also shows that P3HT-*b*-PSSNa block copolymer has a narrow molecular weight distribution.

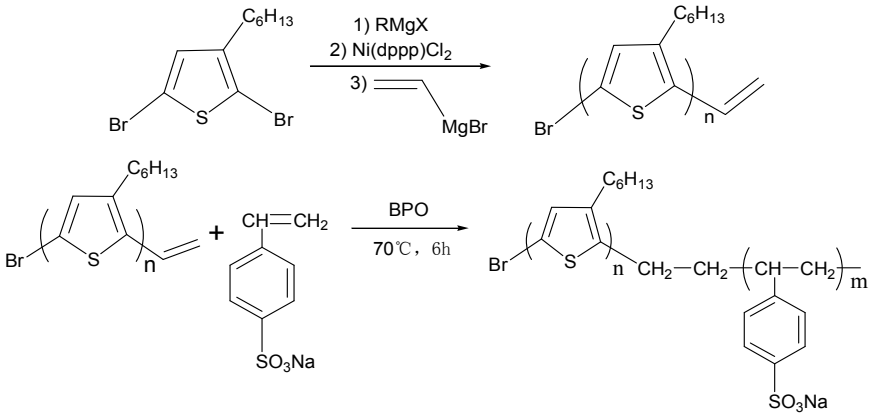

Scheme 1 Synthesis methods of *v*-P3HT and P3HT-*b*-PSSNa

The compositions of block copolymers can be determined from the integral ratio of the signals of P3HT and PSSNa in the ^{1}H NMR spectrum. According to the ^{1}H NMR spectrum of P3HT-*b*-PSSNa, the signal at 8.5~7.5 ppm corresponds to the protons of PSSNa. Thus, the ratios of P3HT and PSSNa segments in P3HT-*b*-PSSNa were determined to be 1:0.2 (named as P3HT-*b*-PSSNa-0.2). P3HT-*b*-PSSNa block copolymer with different ratio can be copolymerized by adding different contents of SSNa monomer, ^{1}H NMR spectra can be seen in the supplementary Figures S1 and S2. The ratios of P3HT and PSSNa segments were 1:0.4 and 1:1.7 (named as P3HT-*b*-PSSNa-0.4 and P3HT-*b*-PSSNa-1.7), respectively. The compositions ratio of P3HT and PSSNa in the block copolymers also can be calculated from the GPC test

and is consistent with the test result of ^{1}H NMR spectrum.

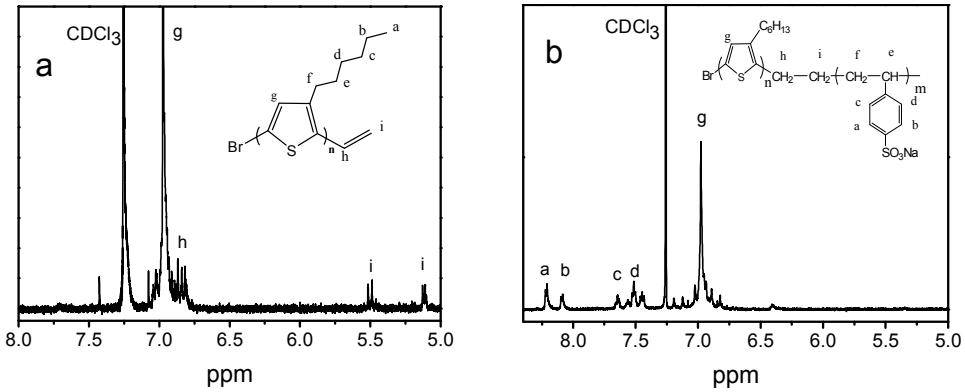

Fig.1 ^{1}HNMR spectrum of *v*-P3HT and P3HT-*b*-PSSNa block copolymer

UV-vis spectra

The as-synthesized P3HT-*b*-PSSNa block copolymers were dispersible in a wide range of solvents because of the amphiphilic nature of the polymers. The solvent effects on the UV-vis absorption of P3HT-*b*-PSSNa block copolymers are shown in Fig.2. Fig.2(a) and Fig.2(b) are the UV-vis absorption spectra of *v*-P3HT and P3HT-*b*-PSSNa in different solutions with the same mixing concentration, respectively. The saturating concentration of polymer is lowered when in a poor solvent. By contrast Fig.2(a) with Fig.2(b), the block polymers show the typical amphiphilic properties. In contrast to the water-insoluble *v*-P3HT, P3HT-*b*-PSSNa exhibits aqueous solubility. The aqueous solubility depends on the PSSNa segment as a proportion of P3HT-*b*-PSSNa. Fig.3 is the photos of *v*-P3HT and P3HT-*b*-PSSNa in different solutions, respectively. The solubilities in different solutions can be observed directly. P3HT-*b*-PSSNa-0.4 has shown the good aqueous solubility in DMF and water in comparison with that of *v*-P3HT. P3HT-*b*-PSSNa-0.4 dissolved in DMF solvent completely and the solution takes on dark red color, and dissolved in water in large part and takes on pink color. For P3HT-*b*-PSSNa-0.2, the solubility is still not have marked improvement in DMF and water (as shown in supplementary Figures S3 and S4).

The UV-vis absorption shift and intensity variation induced by the electronic energy migration along the backbone between adjacent segments (*i.e.*, intrachain) or energy hopping among segments (*i.e.*, interchain) in close proximity.[24] As shown in Fig.2(a) and (b), *v*-P3HT in nonselective good solvents such as chloroform show broad absorption from 300-550 nm. The peak of absorption spectra of the *v*-P3HT is at ca. 430 nm. Which are due to the intrachain π-π* transition of P3HT. The characteristic absorption peaks of P3HT-*b*-PSSNa in chloroform is at ca. 265

nm and ca. 450 nm, respectively, which are corresponding to the π-π* transition of benzene and thiphone rings, respectively. In comparison with *v*-P3HT, the absorption spectra of P3HT-*b*-PSSNa block copolymers show a red shift by ca. 20 nm, which can be ascribed to the incorporation of the doping sulfonic acid group. The molecular chain of polymer tends to be stretched in good solvent and tends to be curled in poor solvent. P3HT with sulfonic acid group has the typical amphiphilic properties and increasing the solubility in different solution. This is in favor of macromolecule chain stretching in the solution and a better coplanar molecular structure. Especially, P3HT-*b*-PSSNa-0.4 show a broad extended absorption edge from 550 nm to 650 nm in chloroform and THF, this indicates that P3HT-*b*-PSSNa-0.4 have stronger electronic coupling and π-π* interactions in chloroform and THF solution.

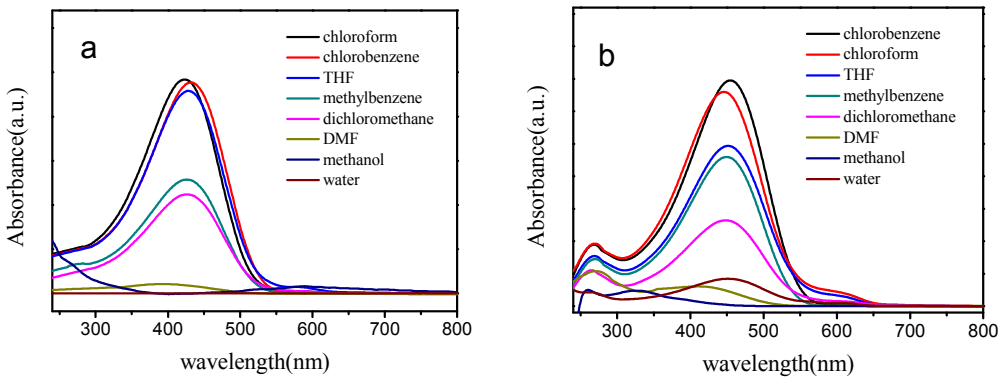

Fig.2 UV-vis spectra of *v*-P3HT(a) and P3HT-*b*-PSSNa-0.4(b) in different solutions

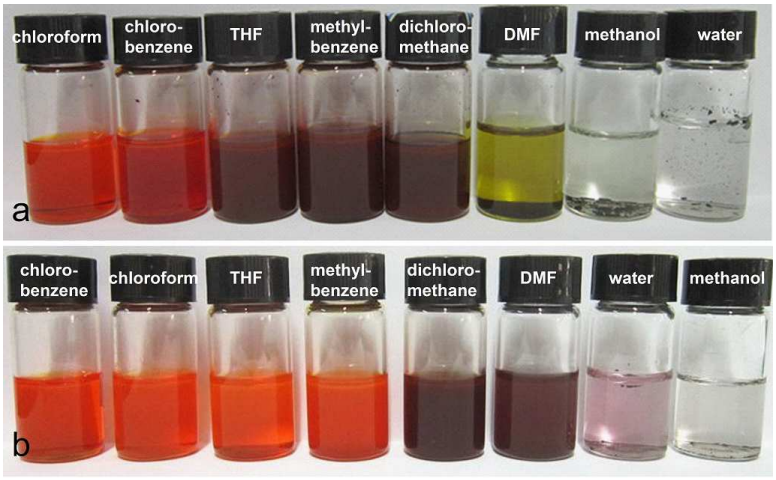

Fig.3 photos of *v*-P3HT (a) and P3HT-b-PSSNa-0.4 (b) in different solvents

The UV-vis spectra of *v*-P3HT and P3HT-*b*-PSSNa solutions and films are shown in fig.4. The UV-vis spectra of *v*-P3HT and P3HT-*b*-PSSNa in the film phase are all turned to broad and depicted a red shift from their solutions. This could be ascribed to

conformational changes increasing the degree of conjugation in the crystalline polymer backbone of the condensed state. P3HT-*b*-PSSNa film shows the broader absorption than that of *v*-P3HT, and the maximum absorption wavelength has a red shifted about 42 nm. It can be described to the increase of effective conjugation length of the polymer chain. Meanwhile, P3HT-*b*-PSSNa block copolymer segment alignment occurs more easily and tends to more regular structure.

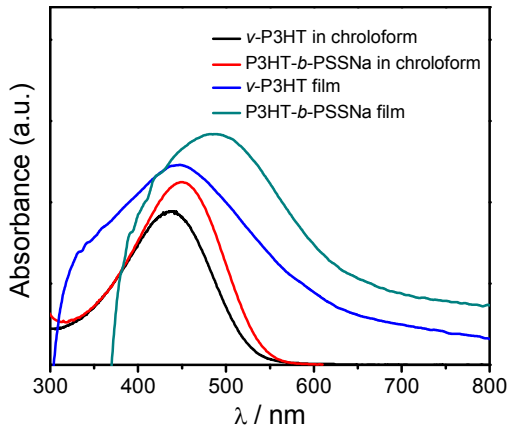

Fig.4 UV-vis spectra of *v*-P3HT and P3HT-*b*-PSSNa-0.2 block copolymer

Electrochemical analysis

The electrochemical properties of *v*-P3HT and P3HT-*b*-PSSNa were investigated using cyclic voltammetry. Fig.5 depicts the CV curves of both the p-doping and n-doping processes. During the cathodic scan, the potiential value of P3HT-*b*-PSSNa shifted with different amounts of SSNa units. The reduction onset potential of P3HT-*b*-PSSNa are in the range of -0.83～-0.95 eV, which are smaller than that of *v*-P3HT. It is noted that the reduction of these block copolymers is more facile than that electron-donating *v*-P3HT due to the presence of doping sulfonate unit, i.e. the copolymer exhibited better electron-transporting properties. The electron affinity (E_a) of these copolymers are higher than that of *v*-P3HT (E_a=3.71eV). This may be attributed to the presence of electron-withdrawing doping moieties in the polymer backbone which decreases the lowest unoccupied molecular orbital (LUMO). Consequently, these copolymers may provide for more facile electron injections when used as active material in photoelectric devices. The n-doping of copolymers were accompanied by an obvious color change (electro-chromism) from dark blue to orange in the n-doping polymers films. In addition, all polymers showed a similar p-doping process. The oxidation peak value are in the range of 0.75～1.76 eV for P3HT-*b*-PSSNa. The oxidation onset potentials of P3HT-*b*-PSSNa decrease in turn may be attributed to the introduction of PSSNa segment, the asymmetry causes oxidation initiation potential turns to the negative shift. P3HT-b-PSSNa-0.4 has the

minimum potential and shows easy to be oxidized. With the increase in the proportion of PSSNa segments, conjugation and electron-withdrawing effects are dominated, and they lead to the oxidation potentials shift positively. During the oxidation process, the color of P3HT-*b*-PSSNa films changed from orange in the original films to dark blue.

The band gap of the copolymer could be estimated from the different of onset potential between the reduction and oxidation processes. The highest occupied molecular orbital (HOMO) and the LUMO are calculated according to the equations reported by de Leeuw et al.[25] : E_{HOMO} = - ($E_{onset,ox}$+4.68eV) and E_{LUMO} = - ($E_{onset,red}$ +4.68eV), where $E_{onset,ox}$ and $E_{onset,red}$ are the onset potentials for the oxidation and reduction versus Ag/AgCl. The cyclic voltammograms of *v*-P3HT and P3HT-*b*-PSSNa are summarized in Table 1. In comparison to *v*-P3HT, P3HT-*b*-PSSNa self-doping copolymers have lower band gap and lower HOMO energy. The band gap of *v*-P3HT is 1.92eV, and the band gap of the P3HT-*b*-PSSNa block copolymer are in the range of 1.61～1.75 eV. It is due to the introduction of the self-doping styrene sulfonate segments which are improve the efficiency of the charge transfer at the D/A interface according to the results above. The beneficial point associated with lower HOMO energy of the self-doping P3HT-*b*-PSSNa copolymers is the advantage of higher open circuit voltage (V_{oc}) of photovoltaic devices.[26]

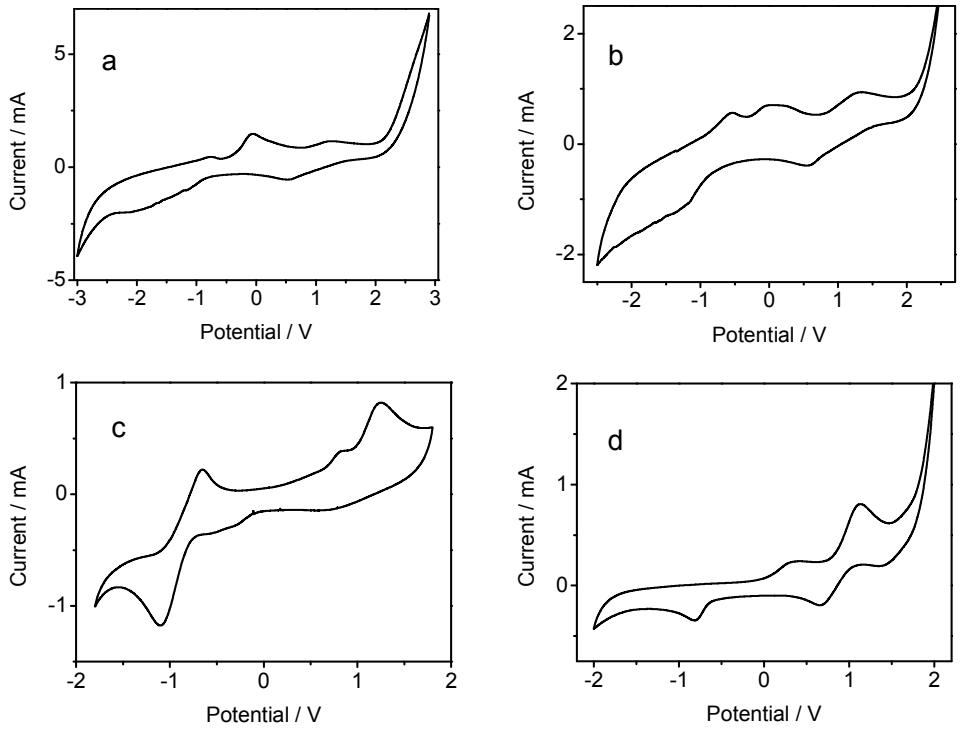

Fig.5 cyclic voltammogram of *v*-P3HT(a) and the block copolymers of P3HT-*b*-PSSNa-0.2 (b), P3HT-*b*-PSSNa-0.4 (c), P3HT-*b*-PSSNa-1.7 (d)

Table 1 Summary of Redox Properties of Various Polymers

Polymer	E_{onset}^{ox}	E_{HOMO}(eV)	I_p(eV)	E_{onset}^{red}	E_{LUMO}(eV)	E_a(eV)	E_g^{ec}(eV)
v-P3HT	0.95	-5.63	5.63	-0.97	-3.71	3.71	1.92
P3HT-*b*-PSSNa-0.2	0.76	-5.44	5.44	-0.95	-3.73	3.73	1.71
P3HT-*b*-PSSNa-0.4	0.75	-5.43	5.43	-0.86	-3.82	3.82	1.61
P3HT-*b*-PSSNa-1.7	0.92	-5.60	5.60	-0.83	-3.85	3.85	1.75

Conducting polymers undergo major physical and chemical changes when oxidized (doped) or reduced (dedoped). These changes are accompanied by charge transference and neutralization processes in electrolyte, involving ion movements to and from the polymer main chains. The proposed mechanism of charge balancing is shown in the Scheme 2. The ‘‘self-doping” in P3HT conducting polymers, in which the anionic group sulfonate attached to the polymer main chain provides rapid charge neutralization and transference when the polymer is electrochemically switched between its oxidation states.[27,28] When the oxidation reaction, thienyl groups with positively charged absorb negatively charged sulfonic acid groups to form intermolecular ion-pairs, whereas the reaction of the reduced state, due to the thienyl groups were not charged, it makes the negatively charged sulfonic acid groups can be left, with reversible doping and de-doping effect.

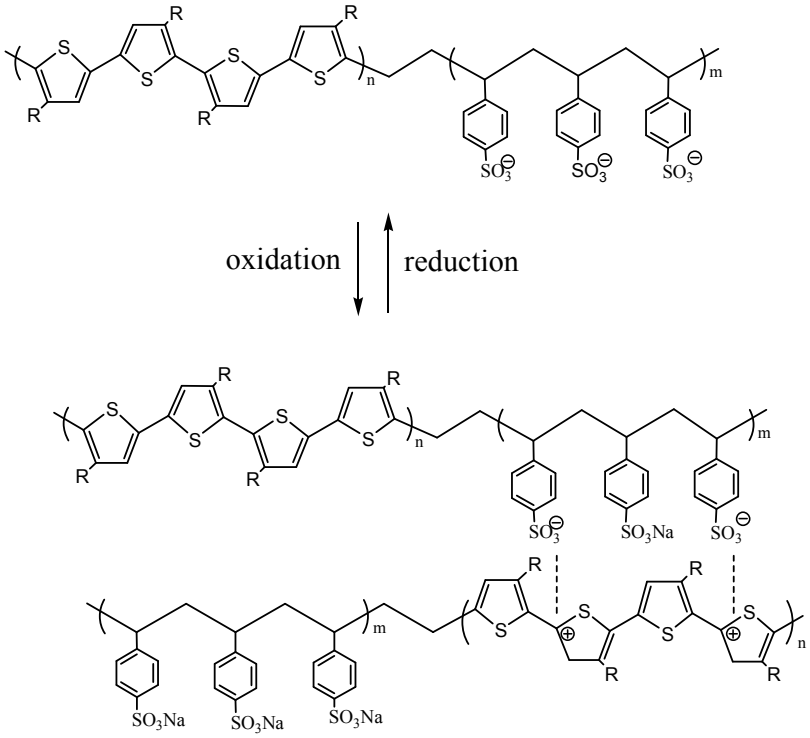

Scheme 2 the doping mechanism of P3HT-b-PSSNa block copolymers

For further understanding, electrochemical impedance of *v*-P3HT and

P3HT-*b*-PSSNa block copolymers were measured in the frequency range of 100 KHz ～ 1 Hz. The impedance spectra are shown as Nyquist plots in Fig.6. A single semicircle in the high frequency region and a straight line in the low frequency region for all spectra can be observed. Base on the Nyquist plots, the equivalent series resistance (ESR) of *v*-P3HT and P3HT-*b*-PSSNa block copolymers obtained from the intersection point of the curves with the axis of real impedance. The difference in the ESR of electrodes can be attributed to the different conductance of electrode materials. The relative low conductivity of *v*-P3HT resulted in the higher charge transfer resistance in it. In comparison, P3HT-*b*-PSSNa block copolymers have the smaller ESR because of their better conductivity. Semi-circular in figure represented the solution resistance and the resistance value of the charge transfer ($R_\Omega + R_\alpha$), since R_Ω of the system can be regarded as fixed values, therefore semi-circular figure could directly compared with the diameter of the semi-circular based R_α. It can be seem from the Nyquist plots that P3HT-*b*-PSSNa block copolymers have the smaller diameter in comparison to that of *v*-P3HT, and P3HT-*b*-PSSNa-0.4 has the smallest diameter among all of the materials, which indicates that P3HT-*b*-PSSNa-0.4 block copolymer had higher conductivity and faster charge transfer rates than the other samples. It is known that the doping-dedoping of polythiophene involves protons, the diffusion process of which often limits the reaction rate. PSSNa is a proton-rich compound with higher proton conductivity. These rich surface-available protons should relieve the diffusion limit imposed by the solution phase for a fast reaction rate.[29]

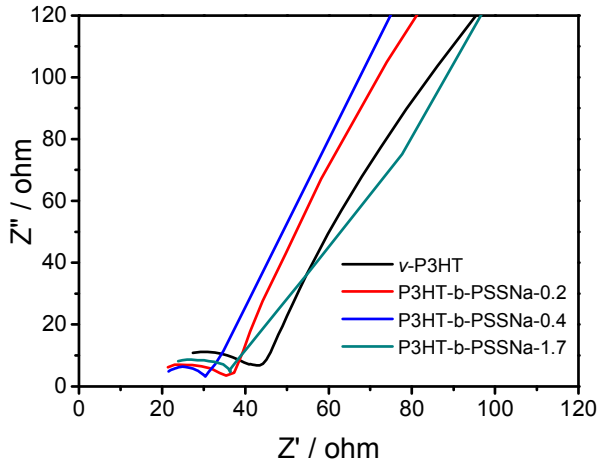

Fig.6 Nyquist curves of *v*-P3HT and P3HT-*b*-PSSNa block copolymer

P3HT-*b*-PSSNa/CdSe blending

The morphologies and structures of CdSe QDs and P3HT-*b*-PSSNa/CdSe blending are shown in Fig.7(a) and (b). The TEM image in Fig.7(a) shows that the CdSe QDs

are uniformity in size and shape. The magnified HRTEM image of CdSe QDs shows a diameter of 4-5 nm and apparent lattice planes can be distinguished. The lattice fringe spacings between two adjacent crystal planes of particles were respectively determined to be 0.214 and 0.213 nm, corresponding to the (202) and (220) planes of CdSe. The CdSe QDs structures have exhibited typical single-crystal features, as revealed by the selected area electron diffraction (SAED) pattern in the inset of Fig.7(b). It has clear diffraction rings that correspond to the cubic phase of CdSe. As shown in Fig.7(b), the CdSe QDs can disperse in the P3HT-*b*-PSSNa polymer matrix uniformly, suggesting a good compatibility between the self-doped conjugated polymer and inorganic CdSe QDs, meanwhile, P3HT-*b*-PSSNa/CdSe blending shows a good film-forming ability in contrast to CdSe QDs. The existence of Se, Cd, S, C and O are evidenced from Energy-dispersive X-ray (EDX) pattern which performed on the surface of the P3HT-*b*-PSSNa/CdSe blending film in Fig.7(c).

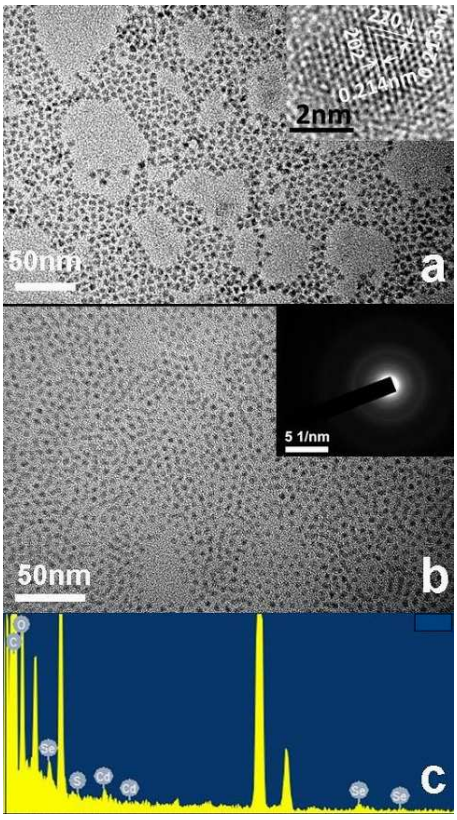

Fig.7 TEM of CdSe QDs (a), inset: magnified HRTEM image of an individual dot; TEM image and EDX pattern of P3HT-*b*-PSSNa/CdSe blending (b, c), inset: the SAED pattern

The charge transfer of different semiconductors in the two-phase D/A interface were studied by means of blending self-doped P3HT-*b*-PSSNa block polymer with CdSe QDs. The UV-vis and PL spectra of P3HT-*b*-PSSNa/CdSe blends are shown in Fig.8. As shown in Fig.8(a), the UV-vis spectrum of P3HT-*b*-PSSNa in chloroform

solution presents a strong absorption peak in the range of 430-450 nm. While the absorption band turned broader and red shifting after blending imcorporation of CdSe QDs, and the absorption intension is increased with increasing the amount of CdSe. It also indicates that P3HT-*b*-PSSNa/CdSe blends have highly efficient light absorption capability in the visible spectrum, which is conducive to better match the solar spectrum. The efficiency of charge generation was further investigated by photoluminescence measurement. As shown in Fig.8(b), it has 35% quenching of photoluminescence occurred at a 1:0.2 mass ratio of P3HT-*b*-PSSNa : CdSe. The quenching of photoluminescence reached 65% at a 1:0.5 mass ratio, and the P3HT-*b*-PSSNa/CdSe blends film shows a nearly complete quenching of more than 95% by a 1:1 mass ratio. The photoluminescence quenching is expected due to the attachment of sulfonic acid dopant to the surface of CdSe because the aromatic π-electrons can act as efficient acceptors for photogenerated holes, thus hindering the radiative recombination process.[30] The high efficiency of quenching can be attributed to the presence of self-doped sulfonic acid groups of P3HT-*b*-PSSNa improved the dispersibility of CdSe QDs in polymer matrix. Which are helpful to the effective charge separate and transfer between the two-phase D/A interface. The highly efficient photoluminescence quenching of P3HT-*b*-PSSNa/CdSe blends suggests that an ultrafast photo-induced charge transfer from P3HT-*b*-PSSNa to CdSe QDs.

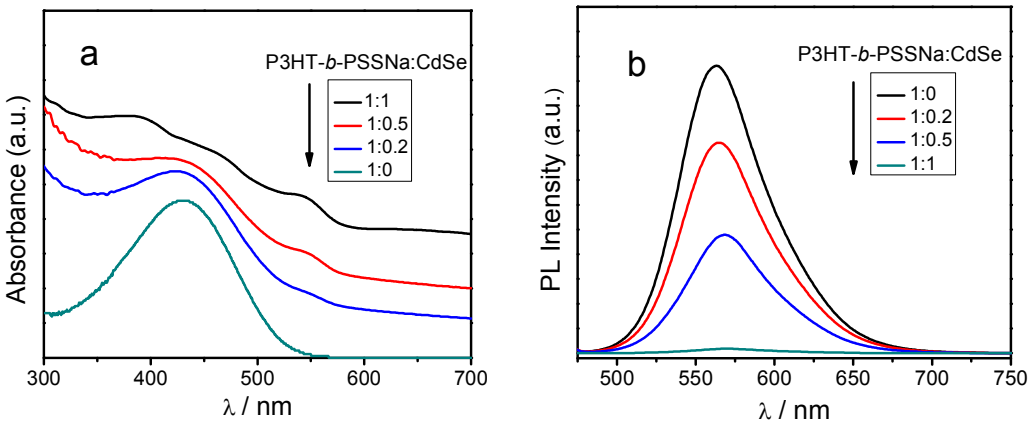

Fig.8 UV-vis (a) and PL spectra (b) of P3HT-*b*-PSSNa/CdSe blend films

The combination between CdSe QDs and P3HT-*b*-PSSNa could be further detected by XPS technique. The XPS patterns of P3HT, P3HT-*b*-PSSNa block copolymer and P3HT-*b*-PSSNa/CdSe blends are presented in Fig.9(a-f), respectively. The energy scales were calibrated by the C1s resonance peak which was fixed to 284.8 eV. Fig.9(a) exhibits the binding energy peak of S2p of the thiophene ring at 164.2 eV and 165.2 eV in bulk P3HT. In Fig.9(b), the peaks at 168.9 eV and 164.4 eV are corresponded to the binding energy of S2p of $-SO_3^-$ group and the thiophene ring,[31]

respectively. It also confirmed the existence of doping -SO_3^-group, and the self-doped P3HT-*b*-PSSNa block copolymer was obtained. The appearance at 532.4 eV in fig.9(c) is ascribed to the binding energy of O1s in -SO_3^-group. In fig.9(d), the peaks at 405.2 eV and 412.0 eV are ascribed to the binding energy of $Cd3d_{5/2}$ and $Cd3d_{3/2}$, respectively.[32] The difference between the two peak positions is 6.8 eV, which is in agreement with the reference.[33] The surface chemical state of Cd is not easy to change in different chemical environment. The chemical bonding between CdSe QDs and P3HT-*b*-PSSNa can be detected from the change of binding energy of S2p. As could be seen in fig.9(e), in comparison with that of S2p of -SO_3^-group, the absence of the peak centered at 168.9 eV in P3HT-*b*-PSSNa illustrated that the S atom in -SO_3^-group has been chemical shifted and may have a combination with CdSe QDs. The further information can be obtained in fig.9(f), the binding energy value of O1s in P3HT-*b*-PSSNa/CdSe blends shows the peaks at 531.9 eV. There is a chemical shift of about 0.5 eV in comparison with that in P3HT-*b*-PSSNa, which means that the surface electronic states of -SO_3^-group in the P3HT-*b*-PSSNa/CdSe blends have been redistributed. That is, -SO_3^-group can doped in P3HT conjugated polymer in one hand, on the other hand the doped -SO_3^-group is in favor for the compatibility with CdSe QDs. The measurement of binding energy provides an evidence for the chemical bonding between CdSe QDs and P3HT-*b*-PSSNa. The XPS results are in coincidence with the morphology observation in TEM images and the photoluminescence quenching between P3HT-*b*-PSSNa and CdSe QDs. The chemical bonding and well dispersion of CdSe QDs in polymer matrix would help photo-generate excitons reaching the D/A interface within their lifetime.

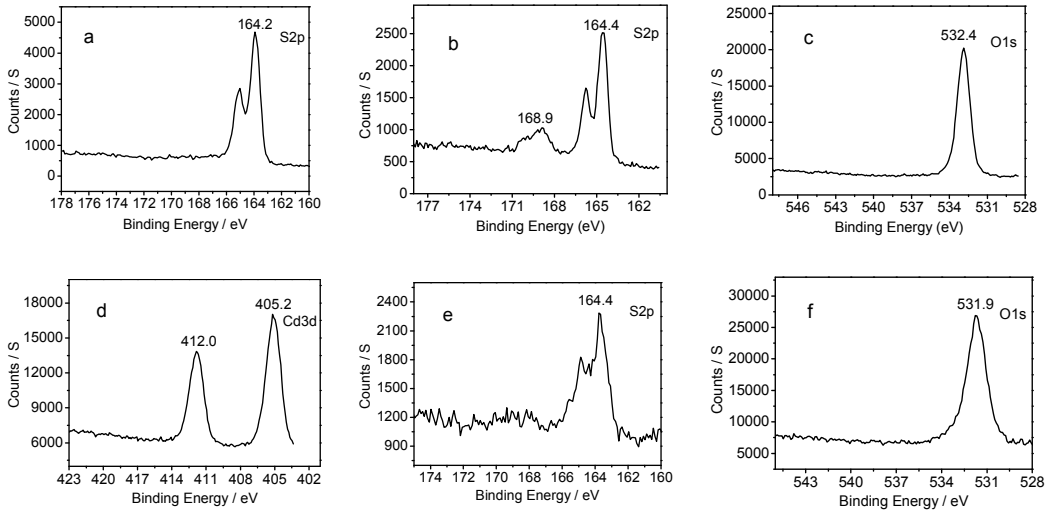

Fig.9 XPS spectra of S2p peak in *v*-P3HT(a), S2p and O1s peaks in P3HT-*b*-PSSNa block copolymer(b, c), Cd3d, S2p and O1s peaks in P3HT-*b*-PSS/CdSe blends(d, e, f)

Conclusions

A new self-doped P3HT-*b*-PSSNa block copolymer was obtained successfully. The segment of P3HT which was synthesized via Grignard metathesis (GRIM) ensures a regular structure and narrow molecular weight distribution. The segment of SSNa which was synthesized via solution copolymerization can be controlled by altering the feed amounts of SSNa monomer, and showing the tunable self-doping and amphiphilic properties. On the one hand, the dopant sulfonic acid groups can improve the conductive properties of conjugated polymer, however, the hydrophilic sulfonic acid groups with longer chain do not help to further increases the conductivity. *v*-P3HT and P3HT-*b*-PSSNa block copolymers all appear sharp reversible peaks corresponding to reversible n-doping and p-doping in cyclic voltammogram, and showing the electrochemical activity. In comparison to *v*-P3HT, P3HT-*b*-PSSNa self-doping copolymers have lower band gap and lower HOMO energy. The self-doping by chemical bonding also can provide a permanent stablity during the alternated thermal and electric cycles. On the other hand, the introduction of sulfonic acid groups improves the solubility of the conjugated polymer in the polar solution and has good compatibility with inorganic QDs. P3HT-*b*-PSSNa show the quite better aqueous solubility in DMF and water in comparison with that of *v*-P3HT. The UV-vis absorption of P3HT-*b*-PSSNa film shows the broader absorption than that of *v*-P3HT, and the maximum absorption wavelength has a red shifted about 42 nm. The characters of good compatibility can greatly increasing the utility of conjugated polymer such as for organic/inorganic hybrid photoelectronic device. In P3HT-*b*-PSSNa/CdSe QDs blending system, CdSe QDs disperses in the P3HT-*b*-PSSNa polymer matrix uniformly, the fluorescence quenching of the copolymer could reached more than 95% when the mass ratio of CdSe QDs and P3HT-*b*-PSSNa copolymer at 1:1. The highly efficient photoluminescence quenching of P3HT-*b*-PSSNa/CdSe blends suggests that an ultrafast photo-induced charge transfer from P3HT-*b*-PSSNa to CdSe QDs.

Acknowledgements

This work was financially supported by National Natural Science Foundation of China (Grant No. 61076040), Anhui Provincial Natural Science Foundation (Grant No. 1208085MB23).

References

[1] I. Osaka and R. D. McCullough, *Acc. Chem. Res.*, 2008, **41**, 1202-1214.

[2] M. Kimura, R.Sakai, S. Sato, T. Fukawa, T. Ikehara, R. Maeda and T. Mihara, *Adv. Funct. Mater.*, 2012, **22**, 469-476.

[3] R. C. Evans, M. Knaapila, N. Willis-Fox, M. Kraft, A. Terry, H. D. Burrows and U. Scherf, *Langmuir*, 2012, **28**, 12348-12356.

[4] C. M. Amb, A. L. Dyer and J. R. Reynolds, *Chem. Mater.*, 2010, **23**, 397-415.

[5] C. B. Nielsen and I. McCulloch, *Prog. Polym. Sci.*, 2013, **38**, 2053-2069.

[6] D. T. McQuade, A. E. Pullen and T. M. Swager, *Chem. Rev.*, 2000, **100**, 2537-2574.

[7] L. V. Lukachova, E. A. Shkerin, E. A. Puganova, E. E. Karyakina, S. G. Kiseleva, A. V. Orlov, G. P. Karpacheva and A. A. Karyakin, *J. Electroanal. Chem.*, 2003, **544**, 59-63.

[8] W. J. Ke, G. H. Lin, C. P. Hsu, C. M. Chen, Y. S. Cheng, T. H. Jen and S. A. Chen, *J. Mater. Chem.*, 2011, **21**, 13483-13489.

[9] J. W. Jung, J. U. Lee and W. H. Jo, *J. Phys. Chem. C*, 2010, **114**, 633-637.

[10] B. D. Martin, J. Naciri, M. H. Moore, A. L. Daniel, A. D. Michael, C. P. Erica and B. Ratna, *Electrochem. Commun.*, 2009, **11**, 169-173.

[11] F. Tran-Van, M. Carrier and C. Chevrot, *Synth. Met.*, 2004, **142**, 251-258.

[12] T. Hirai, S. Osumi, H. Ogawa, T. Hayakawa, A. Takahar, and K. Tanaka, *Macromolecules*, 2014, **47**, 4901-4907.

[13] L. Gao, S. D. Tang, L. Zhu and Genevie`ve Sauve, *Macromolecules*, 2012, **45**, 7404-7412.

[14] J. Yuan, L. Xiao, B. Liu, Y. F. Li, Y. H. He, C. Y. Pan and Y. P. Zou, *J. Mater. Chem. A*, 2013, **1**, 10639-10645.

[15] Y. A. Udum, K. Pekmez and A. Yıldız, *Eur. Polym. J.*, 2005, **41**, 1136-1142.

[16] Y. A. Udum, K. Pekmez and A. Yildiz, *Eur. Polym. J.*, 2004, **40**, 1057-1062.

[17] A. Bruno, C. Borriello, S. A. Haque, C. Minarini and T. D. Luccio, *Phys. Chem. Chem. Phy.*, 2014,**16**, 17998-18003.

[18] J. Y. Lek, G. C. Xing, T. C. Sum and Y. M. Lam, *Appl. Mater. Interfaces*, 2014, **6**, 894–902.

[19] T. T. Xu, M. Yang, J. D. Hoefelmeyer and Q. Q. Qiao, *RSC Advances*, 2012, **2**, 854-862.

[20] S. A. Dowland, L. X. Reynolds, A. MacLachlan, U. B. Cappel and S. A. Haque, *J. Mater. Chem. A*, 2013, **1**, 13896-13901.

[21] J. Wang, X. X. Luo, D. L. Kang, Z. F. Zhou, W. B. Xu and Y. Jian, *J. Nanosci. Nanotechnol.*, 2013, **13**, 523-528.

[22] C. Wang, Y. Jiang, L. Chen, S. Li, G. Li and Z. Zhang, *Macromol. Chem. Phys.*, 2009, **116**, 388-391.

[23] R. D. McCullough, R. D. Lowe, M. Jayaraman and D. L. Anderson, *J. Org. Chem.,* 1993, **58**, 904-912.

[24] E. Collini and G. D. Dcholes, *Science*, 2009, **323**, 369-373.

[25] D. M. de Leeuw, M. M. J. Simenon, A. B. Brown and R. E. F. Einerhand, *Synth. Met.*, 1997, **87**, 53-59.

[26] J. F. Lee, S. L. C. Hsu, P. I. Lee, H. Y. Chuang, M. L. Yang, J. S. Chen and W. Y. Chou, *Sol. Energy Mater. Sol. Cells*, 2011, **95**, 2795-2804.

[27] S. Suematsu, Y. Oura, H. Tsujimoto, H. Kanno and K. Naoi, *Electrochim. Acta*, 2000, **45**, 3813-3821.

[28] F. Tran-Van, M. Carrier and C. Chevrot, *Synth. Met.*, 2004, **142**, 251-258.

[29] Z. M. Cui, C. X. Guo, W. Y. Yuan, C. M. Li, *Phys. Chem. Chem. Phys.*, 2012, **14**, 12823-12828.

[30] K. A. Mazzio, K. Okamoto, Z. Li, S. Gutmann, E. Strein, D. S. Ginger, R. Schlaf and C. K. Luscombe, *Chem. Commun.*, 2013, **49**, 1321-1323.

[31] J. Y. Kim, J. H. Jung, D. E. Lee and J. Joo, *Synth. Met.*, 2002, **126**, 311–316.

[32] J. E. B. Katari, V. L. Colvin and A. P. Alivisatos, *J. Phys. Chem.*, 1994, **98**, 4109-4117.

[33] J. F. Yan, Q. Ye and F. Zhou, *RSC Adv.*, 2012, **2**, 3978-3985.

Captions for Figures

Scheme 1 Synthesis methods of *v*-P3HT and P3HT-*b*-PSSNa

Fig.1 ^{1}HNMR spectrum of *v*-P3HT and P3HT-*b*-PSSNa block copolymer

Fig.2 UV-vis spectra of *v*-P3HT(a) and P3HT-*b*-PSSNa-0.4(b) in different solutions

Fig.3 photos of *v*-P3HT (a) and P3HT-b-PSSNa-0.4 (b) in different solvents

Fig.4 UV-vis spectra of *v*-P3HT and P3HT-*b*-PSSNa-0.2 block copolymer

Fig.5 cyclic voltammogram of *v*-P3HT(a) and the block copolymers of P3HT-*b*-PSSNa-0.2 (b), P3HT-*b*-PSSNa-0.4 (c), P3HT-*b*-PSSNa-1.7 (d)

Scheme 2 the doping mechanism of P3HT-b-PSSNa block copolymers

Fig.6 Nyquist curves of *v*-P3HT and P3HT-*b*-PSSNa block copolymer

Fig.7 TEM of CdSe QDs (a), inset: magnified HRTEM image of an individual dot; TEM image and EDX pattern of P3HT-*b*-PSSNa/CdSe blending (b, c), inset: the SAED pattern

Fig.8 UV-vis (a) and PL spectra (b) of P3HT-*b*-PSSNa/CdSe blend films

Fig.9 XPS spectra of S2p peak in *v*-P3HT(a), S2p and O1s peaks in P3HT-*b*-PSSNa block copolymer(b, c), Cd3d, S2p and O1s peaks in P3HT-*b*-PSS/CdSe blends(d, e, f)

Captions for Tables

Table 1 Summary of Redox Properties of Various Polymers

Only for entry content:

Self-doped 3-hexylthiophene-*b*-sodium styrenesulfonate block copolymer: Synthesis and its organized with CdSe quantum dots

Jin Wang*[a], Chenchen Guo[a], Yongqiang Yu[b], Huabing Yin[c], Xueting Liu[a] and Yang Jiang[d]

A new self-doped 3-hexylthiophene-*b*-Sodium styrenesulfonate block copolymer (P3HT-*b*-PSSNa) was obtained via solution copolymerization of styrene sulfonate (SSNa) with vinyl end group poly (3 - hexylthiophene) (*v*-P3HT) which synthesized under Grignard metathesis (GRIM) reaction conditions. A strategy was developed for producing conjugated polymer with both doped stability during repeated electric cycle and compatibility with inorganic semiconductor materials.

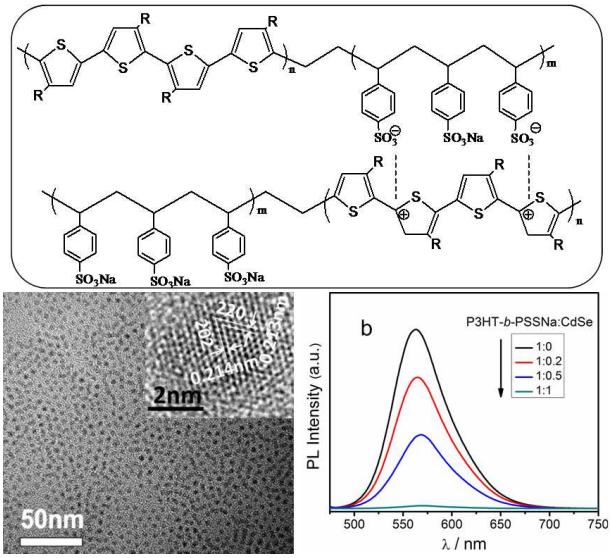

Highlights：

1. Self-doped 3-hexylthiophene-*b*-Sodium styrenesulfonate block copolymer (P3HT-*b*-PSSNa) was synthesized.
2. Chemical bonding and well dispersion of QDs in polymer help photo-generate excitons reaching the D/A interface within their lifetime.
3. Strategy for producing conjugated polymer was developed with both doped stability and compatibility with inorganic semiconductor.